



Simulating carbon accumulation and loss in the central Congo peatlands

Dylan M Young, Andy J Baird, Paul J Morris, Greta C Dargie, Y. Emmanuel Mampouya Wenina, Mackline Mbemba, Arnoud Boom, Peter Cook, Richard Betts, Eleanor Burke, et al.

► To cite this version:

Dylan M Young, Andy J Baird, Paul J Morris, Greta C Dargie, Y. Emmanuel Mampouya Wenina, et al.. Simulating carbon accumulation and loss in the central Congo peatlands. *Global Change Biology*, 2023, 29 (23), pp.6812-6827. 10.1111/gcb.16966 . hal-04320252

HAL Id: hal-04320252

<https://hal.science/hal-04320252>





















Submitted on 4 Dec 2023

HAL is a multi-disciplinary open access archive for the deposit and dissemination of scientific research documents, whether they are published or not. The documents may come from teaching and research institutions in France or abroad, or from public or private research centers.

L'archive ouverte pluridisciplinaire **HAL**, est destinée au dépôt et à la diffusion de documents scientifiques de niveau recherche, publiés ou non, émanant des établissements d'enseignement et de recherche français ou étrangers, des laboratoires publics ou privés.

RESEARCH ARTICLE

Simulating carbon accumulation and loss in the central Congo peatlands

Dylan M. Young¹  | Andy J. Baird¹  | Paul J. Morris¹  | Greta C. Dargie¹  |
 Y. Emmanuel Mampouya Wenina² | Mackline Mbemba² | Arnoud Boom³  |
 Peter Cook⁴  | Richard Betts^{4,5} | Eleanor Burke⁵  | Yannick E. Bocko⁶ |
 Sarah Chadburn⁷ | Dafydd E. Crabtree⁸  | Bart Crezee¹  | Corneille E. N. Ewango^{9,10} |
 Yannick Garcin¹¹  | Selena Georgiou¹²  | Nicholas T. Girkin¹³  | Pauline Gulliver¹⁴ |
 Donna Hawthorne¹⁵  | Suspense A. Ifo² | Ian T. Lawson¹⁵  | Susan E. Page³  |
 A. Jonay Jovani-Sancho^{8,16}  | Enno Schefuß¹⁷  | Matteo Sciumbata¹⁸  |
 Sofie Sjögersten¹⁶  | Simon L. Lewis^{1,19} 

¹School of Geography, University of Leeds, Leeds, UK

²École Normale Supérieure, Département des sciences et vie de la terre, Université Marien Ngouabi, Brazzaville, Republic of the Congo

³School of Geography, Geology and the Environment, University of Leicester, Leicester, UK

⁴Global Systems Institute, University of Exeter, Exeter, UK

⁵Met Office Hadley Centre, Exeter, UK

⁶Faculté des Sciences et Techniques, Université Marien Ngouabi, Brazzaville, Republic of the Congo

⁷College of Engineering, Mathematics, and Physical Sciences, University of Exeter, Exeter, UK

⁸UK Center of Ecology & Hydrology, Bangor, UK

⁹Faculté de Gestion des Ressources Naturelles Renouvelables, Université de Kisangani, Kisangani, Democratic Republic of the Congo

¹⁰Faculté des Sciences, Université de Kisangani, Kisangani, Democratic Republic of the Congo

¹¹CNRS, IRD, INRAE, CEREGE, Aix Marseille University, Aix-en-Provence, France

¹²School of GeoSciences, University of Edinburgh, Edinburgh, UK

¹³School of Water, Energy and Environment, Cranfield University, Cranfield, UK

¹⁴NEIF Radiocarbon Laboratory, Scottish Universities Environmental Research Centre, University of Glasgow, Glasgow, UK

¹⁵School of Geography and Sustainable Development, University of St Andrews, St Andrews, UK

¹⁶School of Biosciences, University of Nottingham, Nottingham, UK

¹⁷MARUM—Center for Marine Environmental Sciences, University of Bremen, Bremen, Germany

¹⁸Amsterdam Institute for Life and Environment, Section Systems Ecology, Vrije Universiteit Amsterdam, Amsterdam, The Netherlands

¹⁹Department of Geography, University College London, London, UK

Correspondence

Dylan M. Young, School of Geography,
University of Leeds, Leeds LS2 9JT, UK.
Email: d.m.young@leeds.ac.uk

Funding information

Natural Environment Research Council,
Grant/Award Number: NE/R016860/1

Abstract

Peatlands of the central Congo Basin have accumulated carbon over millennia. They currently store some 29 billion tonnes of carbon in peat. However, our understanding of the controls on peat carbon accumulation and loss and the vulnerability of this stored carbon to climate change is in its infancy. Here we present a new model of tropical

This is an open access article under the terms of the [Creative Commons Attribution](https://creativecommons.org/licenses/by/4.0/) License, which permits use, distribution and reproduction in any medium, provided the original work is properly cited.

© 2023 The Authors. *Global Change Biology* published by John Wiley & Sons Ltd.

peatland development, DigiBog_Congo, that we use to simulate peat carbon accumulation and loss in a rain-fed interfluvial peatland that began forming ~20,000 calendar years Before Present (cal. yr BP, where 'present' is 1950 CE). Overall, the simulated age-depth curve is in good agreement with palaeoenvironmental reconstructions derived from a peat core at the same location as our model simulation. We find two key controls on long-term peat accumulation: water at the peat surface (surface wetness) and the very slow anoxic decay of recalcitrant material. Our main simulation shows that between the Late Glacial and early Holocene there were several multidecadal periods where net peat and carbon gain alternated with net loss. Later, a climatic dry phase beginning ~5200 cal. yr BP caused the peatland to become a long-term carbon source from ~3975 to 900 cal. yr BP. Peat as old as ~7000 cal. yr BP was decomposed before the peatland's surface became wetter again, suggesting that changes in rainfall alone were sufficient to cause a catastrophic loss of peat carbon lasting thousands of years. During this time, 6.4 m of the column of peat was lost, resulting in 57% of the simulated carbon stock being released. Our study provides an approach to understanding the future impact of climate change and potential land-use change on this vulnerable store of carbon.

KEYWORDS

carbon accumulation, Congo Basin peatlands, palaeoenvironmental reconstruction, simulation, model, tropical peat

1 | INTRODUCTION

The central Congo peatlands, spanning the Democratic Republic of the Congo (DRC) and the Republic of the Congo (ROC), are the

world's largest tropical peatland complex (Dargie et al., 2017) covering 16.8 million ha (Figure 1; Crezee et al., 2022). The peat can be up to 6 m thick (Crezee et al., 2022; Dargie et al., 2017) and in some locations started to accumulate at least around 20,000 years

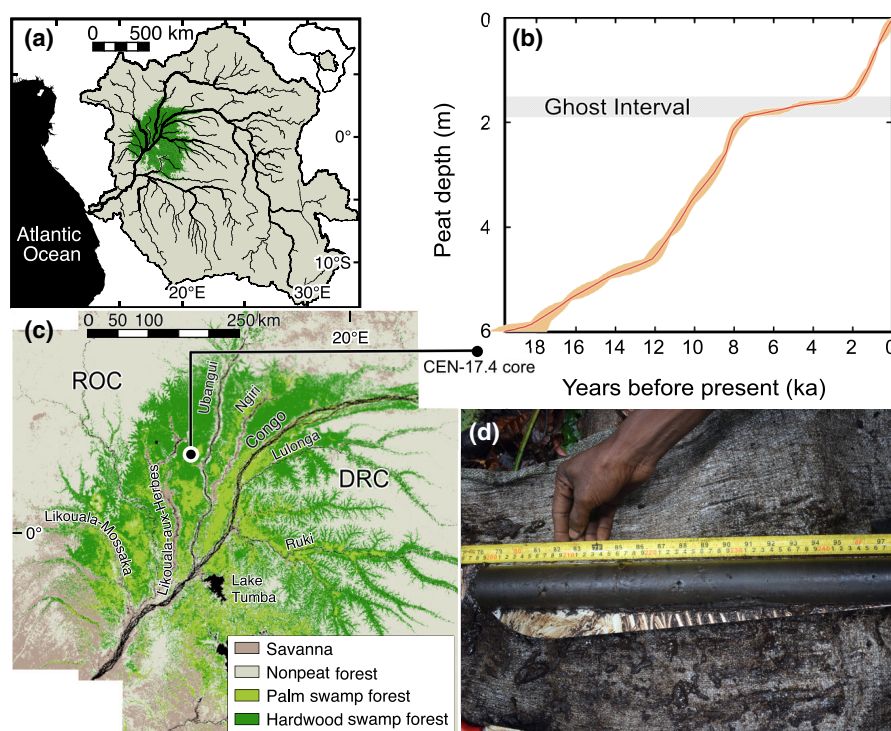


FIGURE 1 Central Congo Basin peatlands and the 'Ghost Interval'. (a) Location of the peatland complex (in green) within the Congo river's drainage basin (in grey). (b) Age-depth curve from a peat core, known as CEN-17.4, showing the Ghost Interval—the thin depth interval highlighted. The red line is the median age modelled at each depth from radiocarbon dates with 95% confidence intervals shown (light red shading). (c) Location within the ROC of the CEN-17.4 coring site. (d) Example of a peat core taken from the peatlands. Maps (a) and (c) from Garcin et al. (2022); data for (b) are from Hawthorne et al. (2023); photograph (d) taken by Bart Crezee. Map lines delineate study areas and do not necessarily depict accepted national boundaries.

ago (Hawthorne et al., 2023). The peatland complex contains an estimated peat carbon stock of 29.0 Pg, equivalent to ~28% of the world's tropical peat carbon (Crezee et al., 2022). As such, the peatlands of the central Congo Basin represent a globally important component of the carbon cycle. The peatlands also appear to be vulnerable to climate change (Garcin et al., 2022) and are under threat from changes in land use, including logging, industrial agriculture and oil exploration and exploitation (Dargie et al., 2019).

Despite their importance, relatively little is known about the genesis, long-term development and vulnerability of the central Congo Basin peatlands, with a detailed palaeo-vegetation analysis available from only one site (Hawthorne et al., 2023). However, recent research has indicated that the carbon stock in these ecosystems appears to be highly sensitive to climatic drying. Using palaeoenvironmental methods to study the past development of these peatlands, Garcin et al. (2022) found evidence of catastrophic loss of peat carbon, caused by centuries of climatic drying that ended ~2000 cal. yr BP. They found the age-depth relationships in peat cores from across the region are shallower in peat dated between ~7500 and ~2000 cal. yr BP than that in older and younger peat. They attributed this feature, which they termed a 'Ghost Interval' (Figure 1), to a late-Holocene reduction in rainfall as evidenced by changes in hydrogen isotope compositions of plant waxes present in the peat. Garcin et al. (2022) proposed that this climatic dry phase led to deepening of peatland water tables and surface drying, exposing thousands of years of accumulated peat to renewed aerobic decomposition. This secondary decay (*sensu* Tipping, 1995) is thought to have led to vertical wasting of peat that shallowed part of the age-depth profiles. Because the peatlands of the central Congo Basin exist in a considerably drier climate than those in Amazonia and Southeast Asia (Garcin et al., 2022), it appears that a relatively modest reduction in rainfall was sufficient to cause a severe loss of peat, tipping them from being a carbon sink to a sustained source.

Several important questions remain about the sensitivity of the peatlands of the central Congo Basin and their carbon stocks to climate change, particularly changes in wetness. First, it is unclear whether rainfall-driven changes in decomposition alone are capable of causing such severe and widespread impacts upon the region's peat and peat carbon stocks, as argued by Garcin et al. (2022), or whether additional factors such as reduced forest productivity, and therefore reduced litter production, also contributed to the Ghost Interval. Second, although the drying and resulting Ghost Interval appears to have been a widespread event that is likely to have caused large losses of peat carbon through enhanced aerobic decay, it is not possible to reconstruct the magnitude or timing of these losses from core-based data alone (Clymo, 1984; Young et al., 2021). Third, it is unclear to what extent the impacts of climatic drying are amplified or buffered by factors such as changes in vegetation composition, peat decomposability and surface water retention. Simulation models of multimillennial peat accumulation and peatland development can be used to address the questions that proxy evidence alone cannot answer. We decided, therefore, to use a model to simulate the

age-depth relationship from the site of the main peat core analysed by Garcin et al. (2022; see also Hawthorne et al., 2023).

Several models of peatland development exist, two of which have been applied in tropical settings, and we considered whether these would be suitable for investigating the central Congo peatland system. The Holocene Peat Model (HPM) has been adapted to simulate palm swamp peat development in Southeast Asia (Frolking et al., 2010; Kurnianto et al., 2015). This tropical version of HPM—HPMTrop—is a cohort-based model that simulates the accumulation of peat by the addition of layers of plant litter (above- and below-ground) that decay depending on the degree of anoxia of each layer. In HPMTrop, water tables are simulated outside of the model using an empirical relationship between water-table depth and a meteorological water deficit (based on rainfall) for a site in the Sebangau swamp forest, Kalimantan, Indonesia. The water-table model always predicts a subsurface water table. However, at our central Congo Basin site, the peat surface was typically inundated during the wet seasons, with lateral water loss occurring predominantly via overland flow (see Sections 2.1 and 2.5).

Cobb et al. (2017) report an alternative model, also applied to peat domes in Southeast Asia. Their unnamed model is based on the Boussinesq groundwater equation and a simple function describing the rate of peatland growth or subsidence using a single peat addition parameter and a single decay coefficient for aerobic decay. Peat addition in the model is assumed to be the same for all plant functional types, and anaerobic decay is assumed to be negligible—that is, it is ignored in the peatland growth function. In essence, a peatland will grow or subside in the Cobb et al. model according to the position of the water table. Although the modelling approach used by Cobb et al. (2017) is attractively simple and leads to interesting inferences about the behaviour of tropical peatland domes, we chose not to use it for two main reasons. First, as we show later (Sections 2.3 and 3.1) we found that decay of different litter/peat fractions at our Congo site did not meet the simple assumptions behind the Cobb et al. (2017) model, in particular that of anaerobic decay not occurring. Second, we wished to develop a model that could account for a range of plant functional types, which may have different productivities and produce litter with differing resistances to decay (Sections 2.2, 2.3 and 3.1). We chose, therefore, to adapt a model that we had already developed for temperate and boreal peatlands: DigiBog (Baird et al., 2012; Morris et al., 2012; Ramirez et al., 2023; Young et al., 2017).

We used the new version of DigiBog—DigiBog_Congo—to simulate the distinctive age-depth curve of the ~20,000-year, 6-m long CEN-17.4 peat core analysed by Garcin et al. (2022) and Hawthorne et al. (2023) (red line, our Figure 1b). The core is from a large (~45 km wide) rain-fed interfluvial basin in the central Congo peatland complex. Our objectives were to:

1. Establish whether rainfall-driven changes in peat decomposition alone can force a model of peatland development to replicate the age-depth curve of the CEN-17.4 core, without extensive parameter tuning.

2. Develop an estimate of how much peat may have been lost during the dry phase that caused the Ghost Interval: Garcin et al. (2022) suggest between 2 and 4 m of peat was lost.
3. Use the model to explore factors that may amplify or buffer the effects of climatic drying on peat accumulation and loss in these globally important carbon stores.

2 | MODEL DESCRIPTION

2.1 | DigiBog_Congo: Modifications for tropical peatland development

DigiBog_Congo incorporates the two main plant functional types (PFTs) of the Congo peatlands—swamp forest hardwood tree and trunkless palm. We improve on previous versions of DigiBog by (1) splitting each PFT into two aboveground litter fractions (leaves and wood) and one belowground fraction (roots), (2) partitioning each fraction into labile and recalcitrant material, (3) modifying the model's decay function so that labile and recalcitrant materials decompose at different rates and (4) including a simple CO₂ fertilisation effect on litter production. We also improved the representation of surface water dynamics by adding a new function for overland flow (Figure 2).

We configured our model as a 1-D representation of the centre of our study site with no lateral subsurface drainage, which for peatlands with a very large lateral extent and small hydraulic gradients is negligible (Section S1). The simulated peatland is a single column that grows upwards as new layers of plant litter are added annually to its surface whilst roots are added to existing peat layers within the shallow subsurface. The column of peat loses mass as all peat layers within it are decomposed subannually at a rate that depends on the

position of the water table and annual air temperature. Whether peat thickness increases or decreases depends on the difference between gains by litter production and losses from peat decay. Recharge is by net rainfall, the difference between rainfall and evapotranspiration: When net rainfall is negative (i.e. when evapotranspiration exceeds rainfall), water is removed from the peatland. In the model, water can also be stored on the peatland surface. Such ponding of surface water is typical during the rainy seasons at the site (Figure 2, Section 2.5).

2.2 | Plant functional types (PFTs) and litter inputs

We simulated two PFTs—a swamp forest hardwood tree and a swamp forest trunkless palm—that, between them, comprise the majority of the vegetation of the central Congo peatlands (Bocko et al., 2023; Crezee et al., 2022; Dargie et al., 2017). Although a recent study has described the past vegetation of the peatland at our study site using pollen data (Hawthorne et al., 2023), we cannot infer from these data the contemporaneous abundance of the species or the mechanisms by which their composition changes. We therefore chose to explore the effect of different proportions of the two main swamp forest PFTs in a sensitivity analysis (Sections 3.3 and 4.2). In the model, each PFT produces surface (leaves and wood) and sub-surface (root) litter, the latter being 'injected' into layers of older, more decayed peat (Barthelmes et al., 2006). In DigiBog_Congo, root inputs are allocated evenly with depth through the rooting zone. We allow root depth to vary with peat thickness until a maximum rooting depth of 30 cm is reached (Figure S1; Table 1; Sciumbata et al., 2023).

Litter input data available from the study site showed no statistical relationship with water-table depth or temperature (Section 3.1): We therefore did not vary litter inputs according to water-table depth

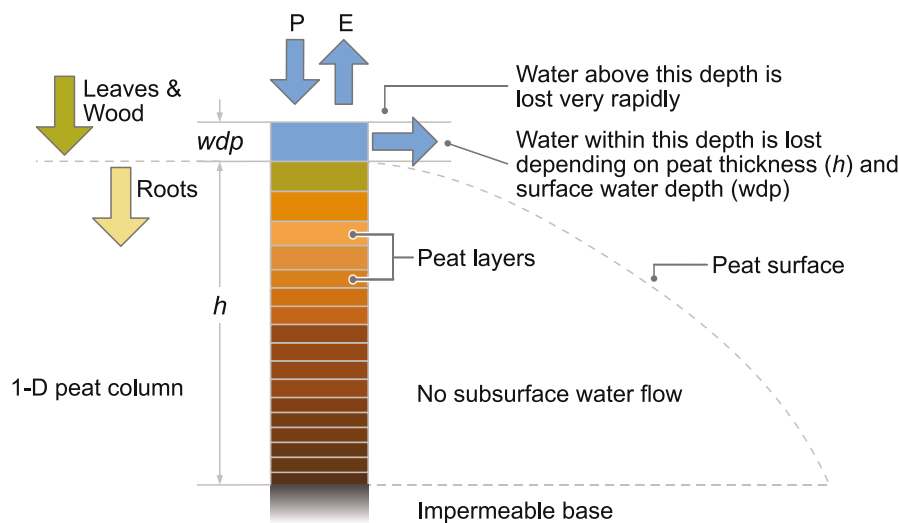


FIGURE 2 Schematic of how DigiBog_Congo is set up to simulate the largely intact interfluvial peatlands in the central Congo Basin. A single column made up of layers of peat increases or loses height because of the balance between plant litter addition (above- and belowground) and peat decay. There is no subsurface drainage. Water is added to, or removed from, the simulated peatland as the difference between net rainfall—(P) minus evapotranspiration (E)—and surface water (blue layer) overland flow losses. Peat decays at different rates depending on the position of the water table, air temperature and the recalcitrance of the litter pools within peat layers (the darker colour indicates a greater degree of decay). Note that the gradient of the peat surface is highly exaggerated.

TABLE 1 Plant functional type parameters and source for main simulation.

Parameter	Palm PFT	Hardwood PFT	Units	Source
Oxic decay (labile and recalcitrant litter pools)				
Leaves oxic decay: labile and recalcitrant	0.18	0.28	prop. year ⁻¹	field data
Wood oxic decay: labile and recalcitrant	0.39	0.2	prop. year ⁻¹	field data
Roots oxic decay: labile and recalcitrant	0.35	0.26	prop. year ⁻¹	field data
Anoxic decay (labile litter pool)				
Leaves anoxic decay: labile	0.05	0.08	prop. year ⁻¹	field data
Wood anoxic decay: labile	0.11	0.03	prop. year ⁻¹	field data
Roots anoxic decay: labile	0.07	0.12	prop. year ⁻¹	field data
Anoxic decay (recalcitrant litter pool)				
Anoxic decay recalcitrant: all fractions	0.0001	0.0001	prop. year ⁻¹	estimated via model testing
Proportion of recalcitrant material (all litter fractions)				
Leaves prop. of recalcitrant material	0.12	0.12	prop.	Chimner and Ewel (2005)
Wood prop. of recalcitrant material	0.4	0.4	prop.	Chimner and Ewel (2005)
Roots prop. of recalcitrant material	0.65	0.65	prop.	Chimner and Ewel (2005)
Litter addition				
Leaves new mass	10	819	g m ⁻² year ⁻¹	field data
Wood new mass	275	283	g m ⁻² year ⁻¹	field data
Roots new mass	556	406	g m ⁻² year ⁻¹	field data
Shared PFT parameters				
Dry bulk density (all litter fractions)	0.17	0.17	g cm ⁻³	Crezee et al. (2022)
Maximum root depth	0.3	0.3	m	Sciumbata et al. (2023)
PFT proportion	0.5	0.5	prop.	—

Note: 'field data' refers to measurements made in the two GEM plots—EKG-02 for hardwood trees and in EKG-03 for palms (see the main text).

Abbreviation: prop., proportion.

adding the mean annual mass of each litter fraction at the beginning of each year. Other studies have found statistically significant variation in plant productivity with water-table depth in tropical swamps. For example, Hirano et al. (2012) report a quadratic relationship between gross primary productivity (GPP) and water-table depth for three peat swamp sites in the upper catchment of the Sebangau River in Central Kalimantan, Indonesia. However, there was considerable scatter in their data, with r^2 ranging from 0.2 to 0.26: see also Mezbahuddin et al. (2014) who report on the effects of water-table depth on net ecosystem productivity from one of these sites.

Moreover, the sites of Hirano et al. (2012) differed considerably in vegetation composition, drainage and burn history from those in the central Congo Basin (Bocko et al., 2023; Dargie et al., 2017; Hawthorne et al., 2023). Two of their sites had previously been logged and contained secondary forest, and the third site was dominated by ferns and sedges. Vegetation and peat at the fern/sedge site had been burned twice within a decade before the GPP measurements. All their sites had been drained using canals, and water tables in one dry season fell to depths of over 150 cm compared with a maximum measured depth at one of the Congo Basin peatland sites of ~85 cm. Thus, our litterfall and water-table observations do not support using these data to parameterise our model. Finally, Chave et al. (2010) show that the rate of litterfall in tropical forests does not depend on forest type or on total annual rainfall.

2.3 | Peat decay and recalcitrance

In nontropical versions of DigiBog, a peat layer decays at a rate according to the position of the water table, air temperature and the oxic and anoxic decay parameters, including a recalcitrance effect (see Clymo, 1984; Morris et al., 2015). It is known that the labile material of tropical swamp plant litter initially decays rapidly, with some fractions being largely lost whilst others are more resistant to decay (Chimner & Ewel, 2005; Hodgkins et al., 2018; Hoyos-Santillan et al., 2015; Sjögersten et al., 2014; Wright et al., 2013). In addition to water-table depth, these decomposition losses depend on the type of plant and the litter fraction (Chimner & Ewel, 2005; Sjögersten et al., 2014). Double exponential decay models have been used to separately represent labile and recalcitrant material (e.g. Chimner & Ewel, 2005), although single exponential decay models have also been used (e.g. Wright et al., 2013).

In DigiBog_Congo, we chose to decay the pools of material within each litter fraction separately (i.e. simulating double exponential decay) by partitioning each litter fraction into labile and recalcitrant pools (Chimner & Ewel, 2005; Hodgkins et al., 2018). We incorporate the slow decay of submerged recalcitrant materials whilst still allowing them to decay quickly if exposed to oxic conditions hundreds or thousands of years after they were added to the peatland (Table 1; Hodgkins et al., 2018; Hoyos-Santillan et al., 2015; Wright et al., 2013).

2.4 | CO₂ fertilisation effect (CFE)

Experiments have shown that plant production and biomass increase with increasing atmospheric CO₂ concentration. β is the relative change in production or biomass for an increase in atmospheric CO₂ concentration of 100ppm (Ainsworth & Long, 2005; Terrer et al., 2019; Wang et al., 2020). Our simulations used litterfall values collected at our study site, under contemporary atmospheric CO₂ concentrations. Therefore, past litter inputs needed to be reduced according to the atmospheric CO₂ concentration at those times. Because our simulations cover a range of atmospheric CO₂ concentration of ~200–300ppm, we chose to implement a simple linear relationship between Δ CO₂ and litter inputs. We assumed that the CO₂ fertilisation effect (CFE) was like that incorporated into well-known land-surface models such as JULES (Joint UK Land Environment Simulator)—a value of β of 17%. We also tested the effect of lower (9%) and higher (35%) values of β for each combination of PFTs (Sections 2.2 and 3.3).

2.5 | Overland and subsurface flow

In our 1-D peatland, shown in Figure 2, the inputs and outputs of water are controlled by the driving data (net rainfall) and the way the model simulates overland flow (loss of surface water). We simulate overland flow according to peat thickness (peatland height) and the depth of water stored on the peatland surface. In previous versions of the model, surface water is lost from the model domain only when a specified depth of water is exceeded. In DigiBog_Congo, our aim was to represent the increasing connectivity of surface water as it deepens, overtopping hollows; and to take account of the increase in gradient between slightly thicker, higher, peat at the dome centre and the margin. Thus, we added a simple, two-part linear equation ($\alpha \times \text{wdp} + (q \times h)$), to simulate water loss from the peatland surface, where wdp is the depth (m) of water stored on the surface, h is the thickness (m) of the peatland above a mineral base, and α and q are constants (Figure 2). To set the initial values of α and q , we experimented with their values to increase overland flow losses as surface water depth increased and the peatland thickened (grew in height).

3 | MODEL PARAMETERISATION AND SET-UP

Four sets of data are needed to run DigiBog_Congo: (1) measurement-based estimates of above- and belowground plant litter production; (2) parameter values for peat decay including for conditions above and below the water table; (3) parameter values for overland flow; and (4) time series of the past climate (rainfall, evapotranspiration and temperature) at the core site to drive the model simulations.

The CEN-17.4 peat core (Garcin et al., 2022; Hawthorne et al., 2023) was obtained from an intact interfluvial peatland near Ekolongouma in the Republic of the Congo (Figure 1). It is a shallow-domed swamp forest peatland ~45km wide (east to west) situated between the Likouala-aux-Herbes and Ubangui rivers and is 308m above sea level (Davenport et al., 2020). Measurements taken along transects of this peatland indicate a maximum peat depth of about 6m, overlying clay and silt, roughly midway between the two rivers (Dargie, 2015; Dargie et al., 2017). Vegetation cover across the transect varies between hardwood trees and trunkless palms (*Raphia laurentii* De Wild; Dargie et al., 2017).

3.1 | Model parameters

In our main model runs, we assume PFT proportions of 50% hardwood tree and 50% palm, but these were varied for the sensitivity analysis. Table 1 shows the model parameters for the different PFTs and their source. Where parameter information was not available from the plot datasets, we searched for it in published studies.

To parameterise the litter inputs, we used 2 years of data collected between March 2019 and March 2021 from two 1ha plots located ~20km from the CEN-17.4 core site. The two plots, representative of a hardwood-dominated (EKG-02) and palm-dominated swamp forest (EKG-03), respectively, were set up and monitored using Global Ecosystem Monitoring (GEM) protocols (Malhi et al., 2021). We used mean annual aboveground leaf litterfall from litter traps for each PFT; mean annual coarse woody inputs collected in ground traps; and root inputs from minirhizotrons (Sciumbata et al., 2023).

To parameterise peat decay, we used data from a replicated litterbag experiment, with litterbags filled with litter fractions from the two PFTs, placed at 0cm (surface) and 50cm depth and decay tracked for 2 years. The two depths represent primarily the effects of oxic and anoxic decay, respectively. The field experiments did not separate litter fractions into labile and recalcitrant pools. We therefore chose to set the oxic decay rate of recalcitrant material to be the same as the oxic decay rate of labile material—evidence suggests that all litter decays rapidly in oxic conditions (Hoyos-Santillan et al., 2015). Because there are currently no data available on the anoxic decay of recalcitrant material from our site or other tropical peatlands, this parameter was estimated from several model runs by comparing the simulated age-depth curve with the core from CEN-17.4.

3.2 | Driving data: The past climate of the central Congo Basin

To drive DigiBog_Congo, we developed a climate reconstruction from 19,600cal. yr BP (the suggested age of basal peat by Hawthorne

et al., 2023) to 0 BP, for a location centred on 18°E, 0°N. We used a combination of palaeoclimate simulations from the HadCM3 global climate model (Valdes et al., 2017) and a proxy reconstruction of annual rainfall (Garcin et al., 2022). The HadCM3 simulations have a three-hour temporal resolution, and we averaged these data into coarser temporal resolutions. We took annual values of air temperature directly from HadCM3, without further alteration. We extracted monthly values of air temperature, humidity, wind speed and net radiation from the HadCM3 simulation and used those to calculate monthly potential evapotranspiration using the Penman–Monteith method (Allen et al., 1998). Garcin et al. (2022) present an annual rainfall reconstruction for our study site; it is based on stable hydrogen isotope compositions in plant waxes and is therefore independent of the age-depth model data from the peat core (see Section S3). We used HadCM3 to superimpose seasonal variability onto this annual reconstruction. To do so, we calculated monthly average rainfall for the period 1001CE (common era) to 2000CE from HadCM3 and expressed each of the twelve monthly averages as a proportion of average annual rainfall during the same period. For each month in our time series, we then estimated monthly rainfall by multiplying the annual estimate from the leaf wax reconstruction (Garcin et al., 2022) by the monthly proportion derived from HadCM3. In this way, the seasonal pattern of rainfall does not change during our reconstruction, even though the annual and monthly totals vary. We chose to use the HadCM3 seasonality from 1001 to 2000CE for the whole rainfall reconstruction (19,600 years) because it resembles more closely that seen in climatic averages from four weather stations in the region (M'puoya, Gambona, Makoua and Ouesso; 1950–1980CE, WMO <https://climatedata-catalogue.wmo.int/explore>) than the long-term trend in the HadCM3 simulation does. Finally, we calculated monthly net rainfall by subtracting monthly potential evapotranspiration from the scaled monthly rainfall values (Figure S2). Because our litter production results showed no relationship with water-table depth, we assume actual evapotranspiration to be equal to potential evapotranspiration. This lack of a relationship suggests the vegetation was not stressed during periods of deeper water tables; that is, leaf stomata would have been open throughout and not limiting CO₂ exchange or transpiration.

3.3 | Sensitivity testing and model evaluation

To constrain DigiBog_Congo, we chose not to tune parameters where empirical data were available and instead carried out a limited sensitivity analysis comprising 21 simulations, namely: (1) the proportions of palm and hardwood trees, which vary across the peatlands; (2) the anoxic decay parameter for recalcitrant material of the root litter fraction; (3) the values for α and q (surface water depth and peat thickness, respectively) in the overland flow equation; and (4) the CO₂ fertilisation effect (CFE) on the different proportions of PFT in (1). We evaluated our simulations by visually assessing the fit of the age-depth curves produced by DigiBog_Congo with that derived from ¹⁴C dated measurements from the CEN-17.4 peat core (Figure 1; Garcin et al., 2022; Hawthorne et al., 2023).

3.3.1 | PFT composition

In the main simulation, we assumed PFT proportions of 50% hardwood and 50% palm. To test the sensitivity of our model to litter inputs from different proportions of the two PFTs, we selected four additional swamp forest compositions that remained constant throughout a simulation: (1) hardwood only; (2) 80% hardwood, 20% palm; (3) 20% hardwood, 80% palm; and (4) palm only.

3.3.2 | Recalcitrant material anoxic decay (roots)

In the main simulation, this was set to 0.0001 year⁻¹ (Table 1). Because we were uncertain about the anoxic decay rate of recalcitrant material, we explored the effect on peat thickness of changing this value to 0.0005 and 0.001 year⁻¹. We also repeated these simulations with low values for the overland flow parameters (α and q were set to 0.001) to assess the effect of changing the recalcitrant material anoxic decay parameter for roots when the peatland surface remains largely saturated.

3.3.3 | CO₂ fertilisation effect

We set β in our main simulation to 17% (i.e. the increase in litterfall for a 100 ppm⁻¹ Δ CO₂). We ran 10 additional simulations using β values of 9% and 35% CFE for each combination of palm and hardwood PFTs. This range encompasses the uncertainty shown in most experiments and Dynamic Global Vegetation Models and satellite-driven estimates (Terrer et al., 2019; Wang et al., 2020). The results of the additional CFE simulations are presented and discussed in the Supporting Information (Section S4).

3.3.4 | Overland flow

In the main simulation, the values were set to $\alpha=0.08$ (the constant applied to surface water depth), $q=0.08$ (the constant applied to peat thickness). Peat accumulation in DigiBog_Congo is very sensitive to surface wetness. We used a single realisation of net rainfall that varied throughout a simulation and therefore did not alter it as part of the sensitivity tests, leaving the parameters α and q in our overland flow function to be used for testing the effects of surface wetness on peatland development. We ran two additional simulations, in the first α was set to 0.15, leaving q equal to 0.08, and for a second run we left α at 0.08 and changed q to 0.15.

4 | RESULTS

We first show the results of our main simulation (50% palm and 50% hardwood PFTs) followed by the results of sensitivity testing.

4.1 | Peat accumulation and loss

Our simulation of the CEN-17.4 site resulted in a final peat thickness for the present day (1950 CE) of 5.72 m (Figure 3d), which is comparable with the CEN-17.4 peat core that has a thickness of 5.99 m. The carbon accumulation rate for the whole simulation, the long-term rate of carbon accumulation (LORCA), is $\sim 25 \text{ g m}^{-2} \text{ year}^{-1}$, similar to the peat core LORCA which is $\sim 26 \text{ g m}^{-2} \text{ year}^{-1}$ (using a dry bulk density of 0.17 g cm^{-3} , Table 1). As importantly for our purposes, the age-depth curve from the peat profile simulated by DigiBog_Congo resembles the measured age-depth curve from the CEN-17.4 peat core (Figure 3d).

Maximum simulated peat thickness was 11.30 m at 3975 cal. yr BP (Figure 3a). After this time, there was a much more prolonged period of drying that caused annual average annual water tables to gradually deepen to 0.19 m by 968 cal. yr BP (Figure 3b shows the 25-year average annual water-table depth), before returning to the peat surface by ~ 900 cal. yr BP, marking the end of ~ 3100 years of continuous peat loss (Figure 3a). The dry period that caused the CEN-17.4 core Ghost Interval began at ~ 5200 cal. yr BP (similar to that reported by Garcin et al. (2022) as the driving data are similar), ~ 1200 years before the simulated peatland began to thin (Figure 3a). The overall effect of the climatic drying on peat stocks was severe: after 3975 cal. yr BP, during the period of enhanced decay, peat thickness was reduced by 6.42 m; i.e. from 11.3 m to ~ 4.9 m. Strikingly, this loss is just over half of the peat that had accumulated before the dry phase.

Based on their plant-wax data, Garcin et al. (2022) estimate the reduction in rainfall that caused secondary peat decay ended ~ 2000 cal. yr BP. At this time, they suggest net peat accumulation resumed because either (1) as the peatland thinned, water losses eventually stabilised and shallower water tables caused less peat to decay (there was a positive NCB) even though conditions remained dry until ~ 800 cal. yr BP; or (2) although there was less total annual rainfall, seasonality decreased enabling the peat surface to become wetter and NCB became positive again. DigiBog_Congo simulates

net peat loss after ~ 2000 cal. yr BP because the simulated annual water table averaged ~ 0.05 m (below the peat surface) from 2000 to 900 cal. yr BP. Between 900 cal. yr BP and the present (1950 CE), the simulated annual water table was, on average, just above the peatland surface (~ 0.11 m). During this time, the peat thickness increased by 0.84 m (Figure 3a).

4.2 | Model sensitivity testing

4.2.1 | PFT composition (Figure 4, sensitivity test 1)

Altering the proportions of PFT in the model did not substantially change the amount of peat accumulation (Figure 4a). Overall, the 100% hardwood tree simulation accumulated 5.98 m of peat by the present day (0 cal. yr BP, 1950 CE) and the 100% palm simulation accumulated 5.48 m during the same period. Before the main period of peat loss, starting at ~ 4000 cal. yr BP, hardwood tree peat was 11.68 m thick whereas palm tree peat was 11.03 m thick. At the end of the period of peat loss (~ 900 cal. yr BP), the monodominant hardwood simulation lost 6.4 m (54.8%) of peat whereas the monodominant palm simulation lost 6.3 m (57.1%). The values of peat accumulation and loss from the 100% hardwood and 100% palm and the age-depth curves of the simulations are broadly similar to each other. The age-depth profiles from the simulations and the CEN-17.4 core are also alike, including the flattening of the age-depth curve that denotes the Ghost Interval (Figure 4b).

4.2.2 | Recalcitrant material anoxic decay (roots) (Figure 4, sensitivity test 2)

Modifying the recalcitrant anoxic decay parameter of the root litter fraction had a marked effect on simulated carbon accumulation rates. The final peat heights of 4.98 m (anoxic decay recalcitrance

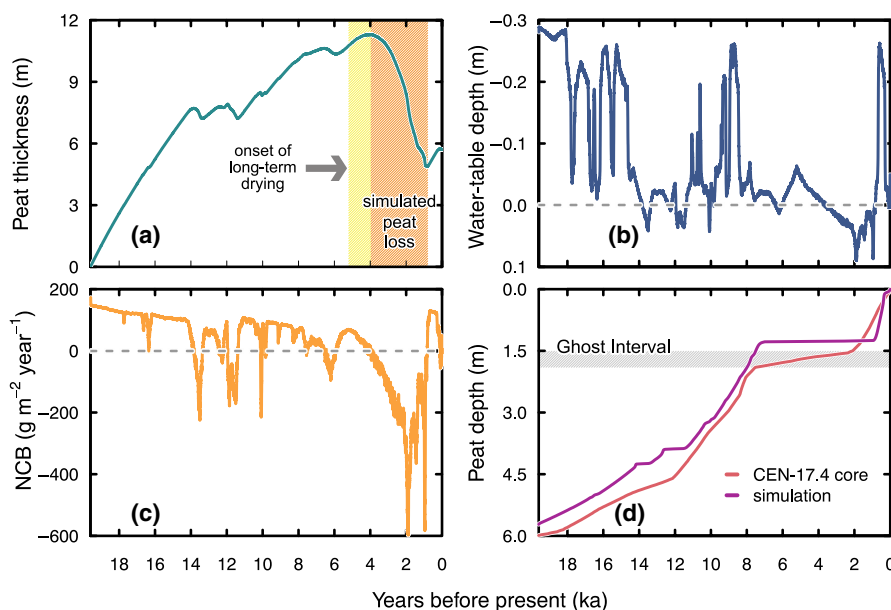


FIGURE 3 Simulated peatland development in the central Congo Basin (main simulation). The vegetation is made up of 50:50 palm and hardwood trees. (a) Annual peat thickness showing the onset of long-term drying (yellow shading) and the period of continuous peat loss (orange shading). (b) 25-year average water-table depth (negative denotes water levels above the ground surface). (c) 25-year average net carbon balance (NCB)—the simulated net carbon accumulation rate. (d) Comparison of the reconstructed and simulated age-depth curves showing the Ghost Interval from the CEN-17.4 peat core (grey shading). The simulation ran for 19,600 years.

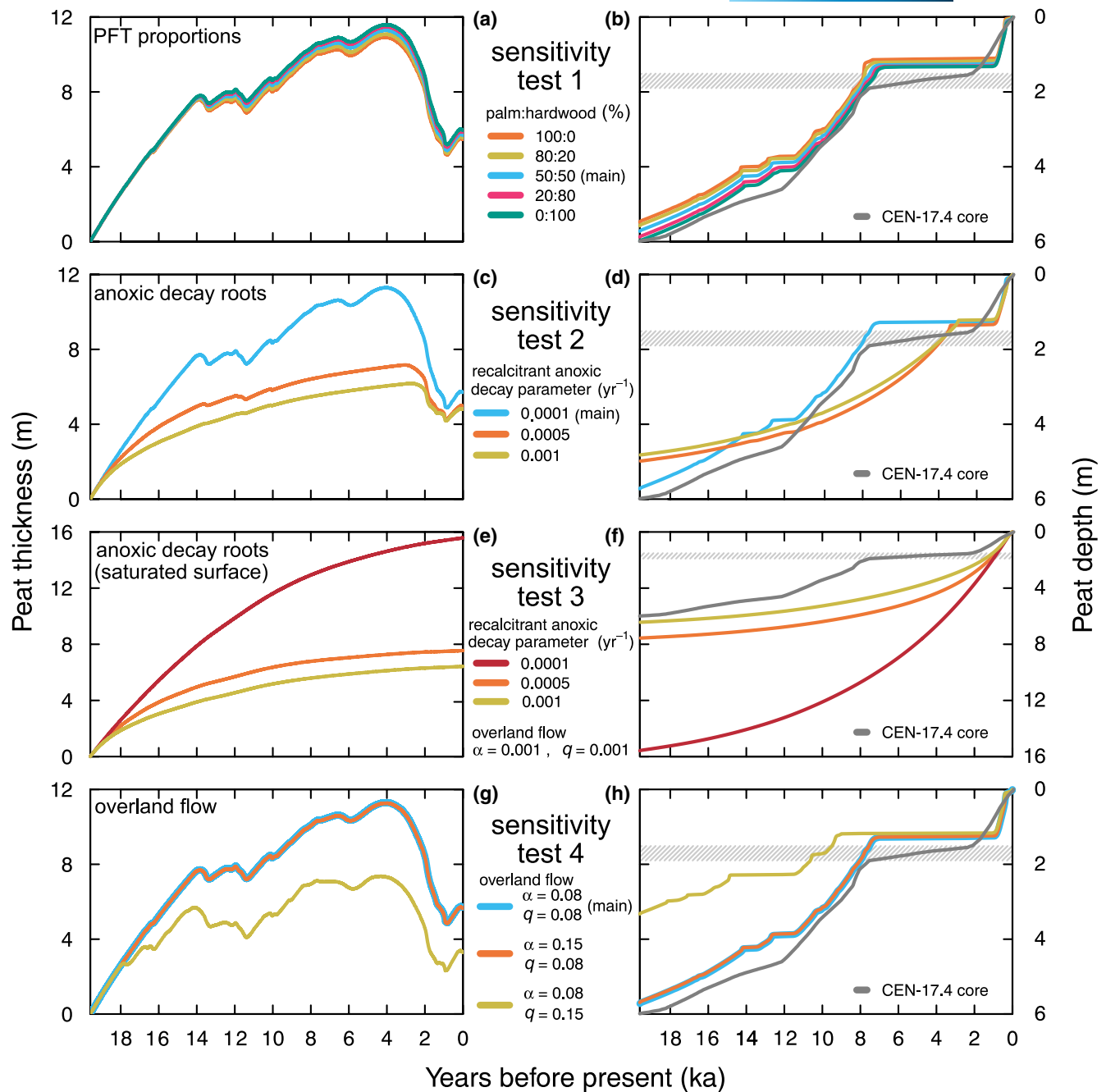


FIGURE 4 Model sensitivity tests. Results are presented in horizontal pairs of panels for each sensitivity test. The legend for each sensitivity test is between each pair. Simulated peat thickness is shown in the left panels, and in the right panels, the simulated age-depth curves are compared with the one from the CEN-17.4 peat core (Garcin et al., 2022). The Ghost Interval is indicated by the horizontal grey shading. Sensitivity test 1, (a) and (b), the proportion of palm and hardwood PFTs; sensitivity test 2, (c) and (d), the anoxic decay parameter of recalcitrant root material; sensitivity test 3, (e) and (f), the anoxic decay parameter of recalcitrant root material when the peat surface remains largely saturated (setting very small overland flow parameter values effectively means water is added or removed from the simulation via net rainfall only); and sensitivity test 4, (g) and (h), changes in the overland flow parameters (α is the depth of surface water and q is peat thickness). Overland flow losses increase as these values increase. Note that in panels (g) and (h), the orange line (where overland flow was increased as the depth of surface water increased, α) overplots the blue line of the main simulation.

roots of 0.0005year^{-1}) and 4.82m (anoxic decay recalcitrance roots of 0.001year^{-1}) are thinner than the CEN-17.4 core (5.99m), and maximum peat thicknesses were 7.16m and 6.18m, respectively (Figure 4c). Because the recalcitrant material of root litter decays more readily than in the main simulation (0.0001year^{-1} , peat

thickness is 11.3m), these thicknesses are 6.32m and 6.48m thinner before continuous peat loss begins at ~3400 and 2742 cal. yr BP, respectively (~700 to ~1400 years later than the main simulation). As a result, the simulated and reconstructed CEN-17.4 core age-depth curves do not closely match (Figure 4d).

4.2.3 | Recalcitrant material anoxic decay (roots) with a saturated peat surface (Figure 4, sensitivity test 3)

We ran two simulations increasing the anoxic decay parameter of roots from 0.0001 year^{-1} to 0.0005 year^{-1} and 0.001 year^{-1} , whilst also setting the overland flow parameters to maintain a saturated peat surface (α and q were 0.001 instead of 0.08. α acts on surface water depth and q acts on peat thickness). In both cases, peat was thicker (7.56 and 6.43 m, Figure 4e) than the measured CEN-17.4 core (5.99 m). Furthermore, there was no evidence of a flattening of the age-depth curves (Figure 4f) seen in the core. The result when the anoxic decay parameter for roots was 0.001 year^{-1} demonstrates that a final simulated thickness (6.18 m) can be similar to the observed thickness (5.99 m), but the age-depth curve does not match (Figure 4e,f).

Finally, for this sensitivity test, we ran a third simulation where anoxic decay of recalcitrant material was very slow (0.0001 year^{-1} , the same as the main simulation) but with almost no overland flow (α and q were very small, 0.001). In this case, the peat surface remained wet allowing peat thickness to increase throughout the model run to 15.6 m, with no evidence of a flattening of the age-depth curve (Figure 4e,f). The mean annual water-table depth for this model run was -0.29 m (above the peat surface), whereas for the main simulation it was -0.07 m . This set of results suggests the very slow decay of recalcitrant material is key to peat accumulation in the Congo peatlands.

4.2.4 | Overland flow (Figure 4, sensitivity test 4)

We further assessed the effect of modifying the constants α and q . For one model run, we set α to 0.15, leaving q equal to 0.08 (both were 0.08 in the main simulation), and for a second simulation, we left α at 0.08 and modified q to 0.15. In comparison with the main simulation, the former modification increases water losses as the surface water deepens, whilst the latter increases surface water losses as the peatland thickens. As expected, increasing the rate at which overland flow losses increase as peat thickness increases (peatland height; $\alpha=0.08$, $q=0.15$) causes less peat to build up during a model run because surface water loss is greater. Increasing the value of α made little change to the main results but when q is almost doubled, the final peat thickness is reduced to 3.33 m, reaching a maximum of 7.37 m before the prolonged dry phase (Figure 4g). Although a pronounced flattening of the age-depth curve is seen (Figure 4h), it extends into peat aged around 9000 cal. yr BP (peat decomposition in the main simulation extends to ~7000 cal. yr BP) because of peat loss of 4.04 m meaning the modelled age-depth curve does not match the one from the CEN-17.4 core. These simulations suggest that surface wetness is a second highly important factor for long-term peat accumulation in the Congo peatlands.

5 | DISCUSSION

Our modelling provides new insights into past peat accumulation and loss in the central Congo peatlands. We were able to constrain our model with empirical data, which were used to inform the model's structure and determine its parameter sets. When driving our model with reconstructed climate for the location of the CEN-17.4 core, we find that peat depth at the present day and the shape of the age-depth curve from our main simulation resemble the empirical data from the peat core (Figure 3).

5.1 | Drivers of long-term net carbon accumulation

Our results reveal two tightly coupled drivers of long-term net carbon accumulation, and therefore peat build-up or loss, in the rain-fed peatlands of the central Congo Basin: surface wetness and the rate of decay of recalcitrant litter (Figure 5). Whilst both have been individually highlighted before (Chimner & Ewel, 2005; Hodgkins et al., 2018; Hoyos-Santillan et al., 2015; Wright et al., 2013), we demonstrate their combined importance on tropical peat accumulation over millennia.

5.1.1 | Surface wetness

Surface wetness is determined by the balance of all of the simulated peatland's inputs and outputs of water, which in our model occur via net rainfall and overland flow. Although average total litter inputs are large ($\sim 12\text{ Mg dry mass ha}^{-1}\text{ year}^{-1}$), when water tables are below the surface both labile and recalcitrant material decay rapidly—within a range of $\sim 20\%$ to $\sim 40\%\text{ year}^{-1}$ (Table 1). Therefore, if the time water tables spend below the peatland surface increases, peat accumulation dynamics switch from net gain to net loss and, during long periods of climatic drying, significant amounts of centuries-old carbon will be released because of secondary decomposition (Figure 3a,d).

The results of our main simulation of the CEN-17.4 location show the importance of surface wetness: Although a prolonged dry phase began at $\sim 5200\text{ cal. yr BP}$, buffering by surface water delayed ongoing carbon losses until $\sim 4000\text{ cal. yr BP}$. Furthermore, of the peat lost, some was aged up to $\sim 7000\text{ cal. yr BP}$, affected by secondary decomposition (i.e. it had accumulated ~ 3000 years before the drier-climate-driven peat losses began; Figure 3a,d). This highlights the catastrophic effect on peat carbon stocks of deeper water levels that could be caused by draining the peatlands, such as for agriculture, oil exploration or a future drying climate. Although we did not simulate changes in rainfall seasonality, our results suggest that increases in dry-season intensity or length, as have been documented in some datasets for the central Congo region over the past two decades (Feng et al., 2013; Jiang et al., 2019), may reduce surface wetness and increase peat decomposition. Furthermore, CMIP (Coupled Model Intercomparison Project) Phase 6 models indicate

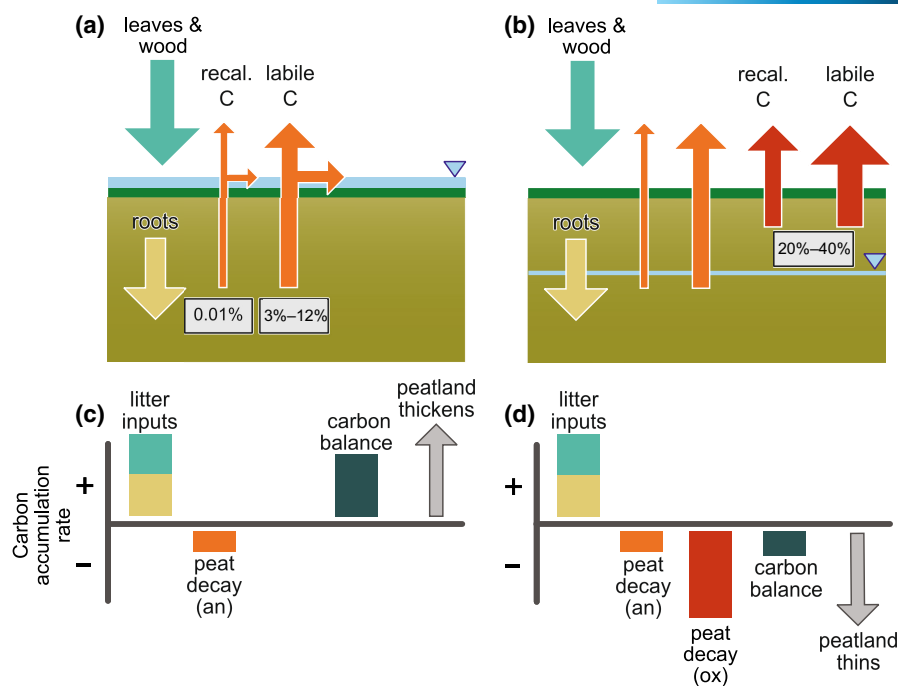


FIGURE 5 Schematic showing the drivers of long-term carbon accumulation in the peatlands of central Congo. (a, b) Above- and belowground inputs are water depth invariant. Sensitivity to surface wetness: (a) Surface inundation—very slow anoxic decay (an) of recalcitrant (recal.) material leads to peat accumulation. (b) Deep water tables—labile and recalcitrant material decay very quickly when exposed to oxic conditions (ox), which results in peat loss. The percentages are the annual proportions of labile and recalcitrant materials lost to decay under oxic and anoxic conditions. (c, d) Carbon balance. (a, b) Arrow size represents the annual proportion of material lost to oxic and anoxic decay processes. The horizontal arrows represent anoxic decay and the stored products of oxic decay lost via overland flow. The inverted blue triangle indicates the water-table position.

an increasing frequency of extreme drought at higher levels of global heating in this region (fig. 4.18 in Caretta et al., 2022).

In large domed peatlands such as the one at CEN-17.4, overland flow is likely to be the main mechanism of water loss: Within-peat lateral drainage is expected to be minimal because of very low hydraulic gradients between the peatland centre and margin (see Section 2.5; Section S1). Therefore, as a domed peatland's centre becomes thicker, and the surface gradient of the peatland increases, overland flow also increases, removing water that protects the upper part of the peat profile from decay. Our simulations suggest that this loss of water can have a significant impact on peat accumulation (Figure 4g). If a peatland's surface remains inundated throughout its development, our results suggest one that is about 20,000 years old could be ~16 m thick (Figure 4e). This value is similar to some peatlands found in Southeast Asia, which occur under a much wetter climate than those in the central Congo Basin (Dommain et al., 2011; Ruwaimana et al., 2020). Whilst 16-m-thick peatlands are unusual in Southeast Asia, the more common less thick peatlands in this region are typically younger than the one we studied in the Congo Basin (e.g. Dommain et al., 2011; Phillips et al., 1997).

The dependency of overland flow rates on peat thickness may also provide a negative feedback mechanism that reduces surface water losses in a domed Congo Basin peatland undergoing peat loss. As the modelled peatland thins, the gradient to the peatland's margin declines and overland flow losses reduce. Therefore, the

peatland's surface may retain more water, causing a reduction in rates of decay in near-surface peat. In other words, the carbon stocks of a thinner peatland, or one that has become thinner, might be less vulnerable in a drier climate because its surface remains wetter. This mechanism may act in a somewhat similar way to the negative feedback that occurs in temperate peatlands when decomposition reduces hydraulic conductivity slowing subsurface drainage (Swindles et al., 2012; Waddington et al., 2015). We suggest that if the net rainfall stabilises, even at a lower level, this feedback could halt peat losses and may allow net peat accumulation to restart. This is consistent with measurements from the CEN-17.4 core where peat accumulation restarted after centuries of peat loss even though the climate remained drier than before the Ghost Interval (Garcin et al., 2022).

Finally, our results also suggest that the peatlands of the central Congo Basin will be vulnerable to land-use change, especially canal and ditch drainage that effectively transforms a peatland into smaller parcels (Cobb et al., 2020, p. 202; Moore et al., 2013). In drained peatlands, hydraulic gradients are much steeper and water losses switch from being mainly overland to mainly subsurface, exposing the upper part of the peat profile to rapid oxic decay until losses stabilise as the peat becomes thinner and in equilibrium with ditch water levels (Baird et al., 2017; Cobb et al., 2020). Evidence from other tropical peatlands has shown that a drying climate and land-use change such as drainage and conversion to oil palm plantations

leads to rapid net losses of carbon due to enhanced decay and fire (Dommain et al., 2014; Konecny et al., 2016; Kurnianto et al., 2019; McCalmont et al., 2021; Miettinen et al., 2017; Moore et al., 2013; Page et al., 2004; Sieffermann et al., 1988). Whilst the impacts of drainage and large-scale agricultural conversion are likely to be common to all tropical peatlands, the Congo peatlands may differ in other respects. For example, given that the Congo peatlands exist in a drier climate than those of tropical Southeast Asia and Amazonia, they may already be more vulnerable to drying (Garcin et al., 2022) without the effects of land-use change.

5.1.2 | Slow anoxic decay of recalcitrant material

Water-saturated labile material decays relatively quickly (3%–12% year⁻¹, Table 1), but all litter fractions contain a proportion of hard-to-decay materials (0.01% year⁻¹ in our main simulation). We show that more rapid rates of anoxic decay of recalcitrant material also result in a peat thickness that is about the same as the CEN-17.4 core after ~20,000 years, but not enough peat accumulates in these parametrisations before the dry phase to produce an age-depth curve similar the one from the CEN-17.4 core (Figure 4c,d). Our simulations suggest that, if the slowly decaying recalcitrant material within the litter fractions remains mostly saturated, there will be long-term peat accumulation (Figure 5).

5.2 | DigiBog_Congo performance

Our main model results compare favourably with the age-depth curve and thickness of the CEN-17.4 peat core. Whilst other combinations of parameters could feasibly produce the same age-depth curve as our main simulation, they are not supported by the field measurements, or the wider tropical peatland literature, that constrain our model. A key reason for the favourable comparison between simulated and observed age-depth curves is that the rainfall reconstruction used to scale our simulated rainfall is derived from leaf waxes from CEN-17.4. We used litterfall and decay input parameters that were not obtained from the CEN-17.4 core and are, therefore, independent of the rainfall reconstruction. Thus, the fit of our main simulation to the observed age-depth curve suggests our model captures the main processes that characterise peat development in the interfluvial rain-fed peatlands of the central Congo Basin.

Ours is the first attempt to model peatland development in the central Congo Basin. However, it is, as yet, unclear how some mechanisms such as the controls on the relative abundance of the PFTs should be simulated, and empirical evidence is not available for some of our model parameters (see Table 1). For example, we lack data on the anoxic decomposition of recalcitrant materials or their proportions within each litter fraction. Improvements to mechanistic understanding, additional litter input field data from other sites and decomposition experiments that include

both labile and recalcitrant litter pools would further constrain our model and likely improve its performance. We also highlight two further datasets needed for model testing at other locations: driving data that include relatively short-lived climate excursions and independent data to compare the simulations with. Accurate palaeo-reconstructions of climate will be needed to simulate the dynamics of past peat accumulation and decomposition. Critically, using HadCM3 rainfall (or many other global reanalysis products) without our locally derived reconstruction would not have produced the patterns of peat accumulation and loss shown in Figure 3a. Additionally, we were able to test DigiBog_Congo by comparing our simulated age-depth curves with the age-depth curve from the CEN-17.4 peat core; therefore, such data will be needed from other locations to assess future model simulations of central Congo peatlands.

5.3 | Ghost Interval: Loss of carbon due to secondary decomposition

The simulations reported here produced an age-depth curve with a flattened section that is similar to the CEN-17.4 age-depth curve (Garcin et al., 2022; Hawthorne et al., 2023). We also simulate a Ghost Interval that is older than the beginning of the dry period, consistent with the hypothesis that it was caused by contemporaneous and secondary decomposition as water tables gradually deepened. The simulated Ghost Interval begins at ~7000 cal. yr BP and ended at 900 cal. yr BP, which is comparable to the radiocarbon dates from CEN-17.4 of ~7500 to ~2000 cal. yr BP, although the simulated Ghost Interval ends closer to the present day than the core (Figure 3d) because annual average water tables remain below the peatland surface until ~900 cal. yr BP. The Ghost Interval in the simulated age-depth curve is flatter than the one from CEN-17.4 (Figure 3d). We investigated this difference: It appears to be because although the simulated annual average water-table depth does not exceed ~0.20 m, the time the water table spends below the surface is greater than the period before the dry phase, eventually causing the NCB to become negative. There could be several reasons for the difference in slope of the Ghost Interval parts of the age-depth curves that are related to the controls on surface wetness and merit investigation in future versions of our model. These are as follows: Our rainfall reconstruction could be too dry, rainfall seasonality may have decreased (one option suggested by Garcin et al., 2022), or we may need to alter our representation of overland flow.

Garcin et al. (2022) estimate the peat lost during the Ghost Interval as between 2.36 and 3.68 m, which is much lower than the 6.42 m of peat loss we simulate, with our result being 74.5%–172.0% higher. The likely reason for this difference is because an age-depth curve from a peat core obtained in the present day does not preserve the accumulation rates from a peatland's developmental history (Young et al., 2021). Our results are consistent with studies of other tropical peatlands, which have also suggested

that a drier climate resulted in the loss of significant amounts of peat, identified by shallow gradients or 'missing sections' in age-depth curves (Kelly et al., 2017; Sieffermann et al., 1988; Wüst et al., 2008). However, using core data alone we can only hypothesise about what happened to a peatland and that includes the CEN-17.4 core. We show how peat core analysis can be taken a key step further by using a peatland development model to help identify what processes are likely to have been responsible for features like the Ghost Interval.

Whilst it is beyond the scope of this paper to estimate total carbon losses associated with the Ghost Interval across the central Congo Basin, these are likely to be large if a similar proportion of peat was lost from all locations within the region. To illustrate the potential magnitude of this change, today the peatlands store 29 Pg C in peat and we estimate that during the Ghost Interval 57% of the peat at the CEN-17.4 location was lost. Yet, when the drying of the climate began at ~5200 cal. yr BP, conditions were wetter than today and the peat we simulate at CEN-17.4 was much thicker. The peatland area may also have been larger, resulting in the central Congo peatlands storing more carbon than in the present day. The maximum peat depth in our main simulation was 11.3 m, which is 5.6 m more than the simulated present-day thickness of 5.7 m. A simple scaling suggests the central Congo peatland complex could have stored twice the amount of carbon in peat than it stores today (~58 Pg C) and therefore may have lost some 33 Pg C during the Ghost Interval. Further work modelling multiple cores from multiple locations will be required to provide robust assessments of the total amount of carbon released to the atmosphere, and its timing, during the Ghost Interval.

6 | CONCLUSIONS

We find that both surface wetness and the slow anoxic decay of recalcitrant material are the main drivers of long-term carbon accumulation in a rain-fed interfluvial central Congo peatland. Our simulations show that the carbon stock of the peatland is highly vulnerable to episodes of climatic drying. More data from the region are required on surface wetness, decomposition rates and the proportion of recalcitrant material within litter fractions, along with rainfall and evapotranspiration records, to understand how future climate change may affect the carbon balance of the peatlands. Our modelling framework can also be used to understand how the potential future exploitation of the central Congo peatlands for timber, industrial agriculture and oil (Dargie et al., 2019) is likely to affect their status as a finely balanced long-term carbon sink.

AUTHOR CONTRIBUTIONS

Dylan M. Young: Data curation; formal analysis; investigation; methodology; software; visualization; writing – original draft; writing – review and editing. **Andy J. Baird:** Conceptualization;

funding acquisition; methodology; project administration; software; supervision; writing – original draft; writing – review and editing. **Paul J. Morris:** Conceptualization; funding acquisition; methodology; software; supervision; writing – original draft; writing – review and editing. **Greta C. Dargie:** Data curation; formal analysis; funding acquisition; investigation; writing – review and editing. **Y. Emmanuel Mampouya Wenina:** Data curation; investigation; writing – review and editing. **Mackline Mbemba:** Data curation; investigation; writing – review and editing. **Arnoud Boom:** Conceptualization; funding acquisition; investigation; resources; writing – review and editing. **Peter Cook:** Formal analysis; writing – original draft; writing – review and editing. **Richard A. Betts:** Funding acquisition; writing – review and editing. **Eleanor Burke:** Resources; writing – review and editing. **Yannick E. Bocko:** Investigation; writing – review and editing. **Sarah Chadburn:** Writing – review and editing. **Dafydd E. Crabtree:** Investigation; writing – review and editing. **Bart Crezee:** Writing – review and editing. **Corneille Ewango:** Funding acquisition; writing – review and editing. **Yannick Garcin:** Resources; writing – original draft; writing – review and editing. **Selena Georgiou:** Writing – review and editing. **Nicholas T. Girkin:** Writing – review and editing. **Pauline Gulliver:** Resources; writing – review and editing. **Donna Hawthorne:** Investigation; writing – review and editing. **Suspense Averti Ifo:** Funding acquisition; writing – review and editing. **Ian Lawson:** Funding acquisition; writing – review and editing. **Susan Page:** Funding acquisition; writing – review and editing. **A. Jonay Jovani-Sancho:** Writing – review and editing. **Enno Schefuß:** Resources; writing – original draft; writing – review and editing. **Matteo Sciumbata:** Investigation; writing – review and editing. **Sofie Sjogersten:** Funding acquisition; writing – review and editing. **Simon L. Lewis:** Conceptualization; funding acquisition; project administration; writing – original draft; writing – review and editing.

ACKNOWLEDGEMENTS

This work was funded by CongoPeat—a NERC large grant (NE/R016860/1) to S.L.L., I.T.L., S.E.P., A.B., A.J.B., P.J.M., P.G. and S.S. Eleanor Burke was supported by the Joint UK BEIS/Defra Met Office Hadley Centre Climate Programme (GA01101). Sarah Chadburn was supported by a Natural Environment Research Council independent research fellowship (grant no. NE/R015791/1). We thank George Biddulph, Lera Miles, Ed Mitchard, the wider CongoPeat network and Richard Rigby for discussions.

CONFLICT OF INTEREST STATEMENT

The authors have no conflict of interest to declare regarding this article.

DATA AVAILABILITY STATEMENT

The model code and input files used for the main simulation reported here are available from: <https://doi.org/10.5281/zenodo.8363948>. The sensitivity tests can be repeated by changing the parameters indicated in the main text.

ORCID

Dylan M. Young  <https://orcid.org/0000-0002-6519-5473>
 Andy J. Baird  <https://orcid.org/0000-0001-8198-3229>
 Paul J. Morris  <https://orcid.org/0000-0002-1145-1478>
 Greta C. Dargie  <https://orcid.org/0000-0002-1871-6360>
 Arnoud Boom  <https://orcid.org/0000-0003-1299-691X>
 Peter Cook  <https://orcid.org/0000-0001-8877-1675>
 Eleanor Burke  <https://orcid.org/0000-0002-2158-141X>
 Dafydd E. Crabtree  <https://orcid.org/0000-0001-7502-8823>
 Bart Crezee  <https://orcid.org/0000-0002-1459-6402>
 Yannick Garcin  <https://orcid.org/0000-0001-8205-494X>
 Selena Georgiou  <https://orcid.org/0000-0002-8865-2948>
 Nicholas T. Girkin  <https://orcid.org/0000-0001-7562-5775>
 Donna Hawthorne  <https://orcid.org/0000-0002-0104-473X>
 Ian T. Lawson  <https://orcid.org/0000-0002-3547-2425>
 Susan E. Page  <https://orcid.org/0000-0002-3392-9241>
 A. Jonay Jovani-Sancho  <https://orcid.org/0000-0002-7824-0501>
 Enno Schefuß  <https://orcid.org/0000-0002-5960-930X>
 Matteo Sciumbata  <https://orcid.org/0000-0001-7189-9568>
 Sofie Sjögersten  <https://orcid.org/0000-0003-4493-1790>
 Simon L. Lewis  <https://orcid.org/0000-0002-8066-6851>

REFERENCES

- Ainsworth, E. A., & Long, S. P. (2005). What have we learned from 15 years of free-air CO₂ enrichment (FACE)? A meta-analytic review of the responses of photosynthesis, canopy properties and plant production to rising CO₂. *New Phytologist*, 165(2), 351–372. <https://doi.org/10.1111/j.1469-8137.2004.01224.x>
- Allen, R. G., Pereira, L. S., Raes, D., & Smith, M. (1998). *Crop evapotranspiration—Guidelines for computing crop water requirements*. FAO Irrigation and Drainage Paper 56, Rome. <http://www.fao.org/docrep/X0490E/X0490E00.htm>
- Baird, A. J., Low, R., Young, D., Swindles, G. T., Lopez, O. R., & Page, S. (2017). High permeability explains the vulnerability of the carbon store in drained tropical peatlands. *Geophysical Research Letters*, 44(3), 1333–1339. <https://doi.org/10.1002/2016GL072245>
- Baird, A. J., Morris, P. J., & Belyea, L. R. (2012). The DigiBog peatland development model 1: Rationale, conceptual model, and hydrological basis. *Ecohydrology*, 5(3), 242–255. <https://doi.org/10.1002/eco.230>
- Barthelmes, A., Prager, A., & Joosten, H. (2006). Palaeoecological analysis of *Alnus* wood peats with special attention to non-pollen palynomorphs. *Review of Palaeobotany and Palynology*, 141(1–2), 33–51. <https://doi.org/10.1016/j.revpalbo.2006.04.002>
- Bocko, Y. E., Panzou, G. J. L., Dargie, G. C., Mampouya, Y. E. W., Mbemba, M., Loumeto, J. J., & Lewis, S. L. (2023). Allometric equation for *Raphia Laurentii* De Wild, the commonest palm in the Central Congo peatlands. *PLoS One*, 18(4), e0273591. <https://doi.org/10.1371/journal.pone.0273591>
- Caretta, M. A., Mukherji, A., Arfanuzzaman, A., Betts, R. A., Gelfan, A., Hirabayashi, Y., Lissner, T. K., Liu, J., Lopez Gunn, E., Morgan, R., Mwanga, S., & Supratid, S. (2022). Water. In H.-O. Pörtner, D. C. Roberts, M. Tignor, E. S. Poloczanska, K. Mintenbeck, A. Alegría, M. Craig, S. Langsdorf, S. Löschke, V. Möller, A. Okem, & B. Rama (Eds.), *Climate change 2022: Impacts, adaptation and vulnerability. Contribution of Working Group II to the sixth assessment report of the Intergovernmental Panel on Climate Change* (pp. 551–712). Cambridge University Press. <https://doi.org/10.1017/9781009325844.006>
- Chave, J., Navarrete, D., Almeida, S., Álvarez, E., Aragão, L. E. O. C., Bonal, D., Châtelet, P., Silva-Espejo, J. E., Goret, J.-Y., von Hildebrand, P., Jiménez, E., Patiño, S., Peñuela, M. C., Phillips, O. L., Stevenson, P., & Malhi, Y. (2010). Regional and seasonal patterns of litterfall in tropical South America. *Biogeosciences*, 7(1), 43–55. <https://doi.org/10.5194/bg-7-43-2010>
- Chimner, R. A., & Ewel, K. C. (2005). A tropical freshwater wetland: II. Production, decomposition, and peat formation. *Wetlands Ecology and Management*, 13(6), 671–684. <https://doi.org/10.1007/s11273-005-0965-9>
- Clymo, R. S. (1984). The limits to peat bog growth. *Philosophical Transactions of the Royal Society of London B: Biological Sciences*, 303(1117), 605–654. <https://doi.org/10.1098/rstb.1984.0002>
- Cobb, A. R., Dommain, R., Tan, F., Heng, N. H. E., & Harvey, C. F. (2020). Carbon storage capacity of tropical peatlands in natural and artificial drainage networks. *Environmental Research Letters*, 15(11), 114009. <https://doi.org/10.1088/1748-9326/aba867>
- Cobb, A. R., Hoyt, A. M., Gandois, L., Eri, J., Dommain, R., Salim, K. A., Kai, F. M., Su'ut, N. S. H., & Harvey, C. F. (2017). How temporal patterns in rainfall determine the geomorphology and carbon fluxes of tropical peatlands. *Proceedings of the National Academy of Sciences of the United States of America*, 114(26), E5187–E5196. <https://doi.org/10.1073/pnas.1701090114>
- Crezee, B., Dargie, G. C., Ewango, C. E. N., Mitchard, E. T. A., Emba, B. O., Kanyama, T. J., Bola, P., Ndjango, J.-B. N., Girkin, N. T., Bocko, Y. E., Ifo, S. A., Hubau, W., Seidensticker, D., Batumike, R., Imani, G., Cuní-Sánchez, A., Kiahtipes, C. A., Lebamba, J., Wotzka, H.-P., ... Lewis, S. L. (2022). Mapping peat thickness and carbon stocks of the Central Congo Basin using field data. *Nature Geoscience*, 15(8), 639–644. <https://doi.org/10.1038/s41561-022-00966-7>
- Dargie, G. C. (2015). *Quantifying and understanding the tropical peatlands of the central Congo Basin* [PhD], University of Leeds. <https://etheses.whiterose.ac.uk/13377/>
- Dargie, G. C., Lawson, I. T., Rayden, T. J., Miles, L., Mitchard, E. T. A., Page, S. E., Bocko, Y. E., Ifo, S. A., & Lewis, S. L. (2019). Congo Basin peatlands: Threats and conservation priorities. *Mitigation and Adaptation Strategies for Global Change*, 24(4), 669–686. <https://doi.org/10.1007/s11027-017-9774-8>
- Dargie, G. C., Lewis, S. L., Lawson, I. T., Mitchard, E. T. A., Page, S. E., Bocko, Y. E., & Ifo, S. A. (2017). Age, extent and carbon storage of the central Congo Basin peatland complex. *Nature*, 542(7639), 86–90. <https://doi.org/10.1038/nature21048>
- Davenport, I. J., McNicol, I., Mitchard, E. T. A., Dargie, G., Suspense, I., Milongo, B., Bocko, Y. E., Hawthorne, D., Lawson, I., Baird, A. J., Page, S., & Lewis, S. L. (2020). First evidence of peat domes in the Congo Basin using LiDAR from a fixed-wing drone. *Remote Sensing*, 12(14), 2196. <https://doi.org/10.3390/rs12142196>
- Dommain, R., Couwenberg, J., Glaser, P. H., Joosten, H., & Suryadiputra, I. N. N. (2014). Carbon storage and release in Indonesian peatlands since the last deglaciation. *Quaternary Science Reviews*, 97, 1–32. <https://doi.org/10.1016/j.quascirev.2014.05.002>
- Dommain, R., Couwenberg, J., & Joosten, H. (2011). Development and carbon sequestration of tropical peat domes in South-East Asia: Links to post-glacial sea-level changes and Holocene climate variability. *Quaternary Science Reviews*, 30(7–8), 999–1010. <https://doi.org/10.1016/j.quascirev.2011.01.018>
- Feng, X., Porporato, A., & Rodriguez-Iturbe, I. (2013). Changes in rainfall seasonality in the tropics. *Nature Climate Change*, 3(9), 811–815. <https://doi.org/10.1038/nclimate1907>
- Frolking, S., Roulet, N. T., Tuittila, E., Bubier, J. L., Quillet, A., Talbot, J., & Richard, P. J. H. (2010). A new model of Holocene peatland net primary production, decomposition, water balance, and peat accumulation. *Earth System Dynamics*, 1(1), 1–21. <https://doi.org/10.5194/esd-1-1-2010>
- Garcin, Y., Schefuß, E., Dargie, G. C., Hawthorne, D., Lawson, I. T., Sebag, D., Biddulph, G. E., Crezee, B., Bocko, Y. E., Ifo, S. A., Mampouya Wenina, Y. E., Mbemba, M., Ewango, C. E. N., Emba, O., Bola, P., Kanyama Tabu, J., Tyrrell, G., Young, D. M., Gassier, G., ... Lewis, S.

- L. (2022). Hydroclimatic vulnerability of peat carbon in the central Congo Basin. *Nature*, 612, 277–282. <https://doi.org/10.1038/s41586-022-05389-3>
- Hawthorne, D., Lawson, I. T., Dargie, G. C., Bocko, Y. E., Ifo, S. A., Garcin, Y., Schefuß, E., Hiles, W., Jovani-Sancho, A. J., Tyrell, G., Biddulph, G. E., Boom, A., Chase, B. M., Gulliver, P., Page, S. E., Roucoux, K. H., Sjögersten, S., Young, D. M., & Lewis, S. L. (2023). Genesis and development of an interfluvial peatland in the central Congo Basin since the Late Pleistocene. *Quaternary Science Reviews*, 305, 107992. <https://doi.org/10.1016/j.quascirev.2023.107992>
- Hirano, T., Segah, H., Kusin, K., Limin, S., Takahashi, H., & Osaki, M. (2012). Effects of disturbances on the carbon balance of tropical peat swamp forests. *Global Change Biology*, 18(11), 3410–3422. <https://doi.org/10.1111/j.1365-2486.2012.02793.x>
- Hodgkins, S. B., Richardson, C. J., Dommain, R., Wang, H., Glaser, P. H., Verbeke, B., Winkler, B. R., Cobb, A. R., Rich, V. I., Missilmani, M., Flanagan, N., Ho, M., Hoyt, A. M., Harvey, C. F., Vining, S. R., Hough, M. A., Moore, T. R., Richard, P. J. H., De La Cruz, F. B., ... Chanton, J. P. (2018). Tropical peatland carbon storage linked to global latitudinal trends in peat recalcitrance. *Nature Communications*, 9(1), 3640. <https://doi.org/10.1038/s41467-018-06050-2>
- Hoyos-Santillan, J., Lomax, B. H., Large, D., Turner, B. L., Boom, A., Lopez, O. R., & Sjögersten, S. (2015). Getting to the root of the problem: Litter decomposition and peat formation in lowland neotropical peatlands. *Biogeochemistry*, 126(1–2), 115–129. <https://doi.org/10.1007/s10533-015-0147-7>
- Jiang, Y., Zhou, L., Tucker, C. J., Raghavendra, A., Hua, W., Liu, Y. Y., & Joiner, J. (2019). Widespread increase of boreal summer dry season length over the Congo rainforest. *Nature Climate Change*, 9(8), 617–622. <https://doi.org/10.1038/s41558-019-0512-y>
- Kelly, T. J., Lawson, I. T., Roucoux, K. H., Baker, T. R., Jones, T. D., & Sanderson, N. K. (2017). The vegetation history of an Amazonian domed peatland. *Palaeogeography, Palaeoclimatology, Palaeoecology*, 468, 129–141. <https://doi.org/10.1016/j.palaeo.2016.11.039>
- Konecny, K., Ballhorn, U., Navratil, P., Jubanski, J., Page, S. E., Tansey, K., Hooijer, A., Vernimmen, R., & Siegert, F. (2016). Variable carbon losses from recurrent fires in drained tropical peatlands. *Global Change Biology*, 22(4), 1469–1480. <https://doi.org/10.1111/gcb.13186>
- Kurnianto, S., Selker, J., Boone Kauffman, J., Murdiyarso, D., & Peterson, J. T. (2019). The influence of land-cover changes on the variability of saturated hydraulic conductivity in tropical peatlands. *Mitigation and Adaptation Strategies for Global Change*, 24(4), 535–555. <https://doi.org/10.1007/s11027-018-9802-3>
- Kurnianto, S., Warren, M., Talbot, J., Kauffman, B., Murdiyarso, D., & Frolking, S. (2015). Carbon accumulation of tropical peatlands over millennia: A modelling approach. *Global Change Biology*, 21(1), 431–444. <https://doi.org/10.1111/gcb.12672>
- Malhi, Y., Girardin, C., Metcalfe, D. B., Doughty, C. E., Aragão, L. E. O. C., Rifai, S. W., Oliveras, I., Shenkin, A., Aguirre-Gutiérrez, J., Dahlsjö, C. A. L., Riutta, T., Berenguer, E., Moore, S., Huasco, W. H., Salinas, N., da Costa, A. C. L., Bentley, L. P., Adu-Bredu, S., Marthews, T. R., ... Phillips, O. L. (2021). The Global Ecosystems Monitoring Network: Monitoring ecosystem productivity and carbon cycling across the tropics. *Biological Conservation*, 253, 108889. <https://doi.org/10.1016/j.biocon.2020.108889>
- McCalmont, J., Kho, L. K., Teh, Y. A., Lewis, K., Chocholek, M., Rumpang, E., & Hill, T. (2021). Short- and long-term carbon emissions from oil palm plantations converted from logged tropical peat swamp forest. *Global Change Biology*, 27(11), 2361–2376. <https://doi.org/10.1111/gcb.15544>
- Mezbahuddin, M., Grant, R. F., & Hirano, T. (2014). Modelling effects of seasonal variation in water table depth on net ecosystem CO₂ exchange of a tropical peatland. *Biogeosciences*, 11(3), 577–599. <https://doi.org/10.5194/bg-11-577-2014>
- Miettinen, J., Hooijer, A., Vernimmen, R., Liew, S. C., & Page, S. E. (2017). From carbon sink to carbon source: Extensive peat oxidation in insular Southeast Asia since 1990. *Environmental Research Letters*, 12(2), 024014. <https://doi.org/10.1088/1748-9326/aa5b6f>
- Moore, S., Evans, C. D., Page, S. E., Garnett, M. H., Jones, T. G., Freeman, C., Hooijer, A., Wiltshire, A. J., Limin, S. H., & Gauci, V. (2013). Deep instability of deforested tropical peatlands revealed by fluvial organic carbon fluxes. *Nature*, 493(7434), 660–663. <https://doi.org/10.1038/nature11818>
- Morris, P. J., Baird, A. J., & Belyea, L. R. (2012). The DigiBog peatland development model 2: Ecohydrological simulations in 2D. *Ecohydrology*, 5(3), 256–268. <https://doi.org/10.1002/eco.229>
- Morris, P. J., Baird, A. J., Young, D. M., & Swindles, G. T. (2015). Untangling climate signals from autogenic changes in long-term peatland development. *Geophysical Research Letters*, 42(24), 2015GL066824. <https://doi.org/10.1002/2015GL066824>
- Page, S. E., Wüst, R. A. J., Weiss, D., Rieley, J. O., Shotyk, W., & Limin, S. H. (2004). A record of Late Pleistocene and Holocene carbon accumulation and climate change from an equatorial peat bog (Kalimantan, Indonesia): Implications for past, present and future carbon dynamics. *Journal of Quaternary Science*, 19(7), 625–635. <https://doi.org/10.1002/jqs.884>
- Phillips, S., Rouse, G. E., & Bustin, R. M. (1997). Vegetation zones and diagnostic pollen profiles of a coastal peat swamp, Bocas del Toro, Panamá. *Palaeogeography, Palaeoclimatology, Palaeoecology*, 128(1–4), 301–338. [https://doi.org/10.1016/S0031-0182\(97\)81129-7](https://doi.org/10.1016/S0031-0182(97)81129-7)
- Ramirez, J. A., Peleg, N., Baird, A. J., Young, D. M., Morris, P. J., Larocque, M., & Garneau, M. (2023). Modelling peatland development in high-boreal Quebec, Canada, with DigiBog_Boreal. *Ecological Modelling*, 478, 110298. <https://doi.org/10.1016/j.ecolmodel.2023.110298>
- Ruwaimana, M., Anshari, G. Z., Silva, L. C. R., & Gavin, D. G. (2020). The oldest extant tropical peatland in the world: A major carbon reservoir for at least 47 000 years. *Environmental Research Letters*, 15(11), 114027. <https://doi.org/10.1088/1748-9326/abb853>
- Sciumbata, M., Wenina, Y. E. M., Mbemba, M., Dargie, G. C., Baird, A. J., Morris, P. J., Ifo, S. A., Aerts, R., & Lewis, S. L. (2023). First estimates of fine root production in tropical peat swamp and terra firme forests of the central Congo Basin. *Scientific Reports*, 13(1), 12315. <https://doi.org/10.1038/s41598-023-38409-x>
- Sieffermann, G., Fournier, M., Triutomo, S., Sadelman, M. T., & Semah, A. M. (1988). Velocity of tropical forest peat accumulation in Central Kalimantan province, Indonesia (Borneo). In *Proceedings VIII International Peat Congress, Leningrad 88, Section I* (pp. 90–98). International Peat Society.
- Sjögersten, S., Black, C. R., Evers, S., Hoyos-Santillan, J., Wright, E. L., & Turner, B. L. (2014). Tropical wetlands: A missing link in the global carbon cycle?: Carbon cycling in tropical wetlands. *Global Biogeochemical Cycles*, 28(12), 1371–1386. <https://doi.org/10.1002/2014GB004844>
- Swindles, G. T., Morris, P. J., Baird, A. J., Blaauw, M., & Plunkett, G. (2012). Ecohydrological feedbacks confound peat-based climate reconstructions. *Geophysical Research Letters*, 39(11), L11401. <https://doi.org/10.1029/2012GL051500>
- Terrer, C., Jackson, R. B., Prentice, I. C., Keenan, T. F., Kaiser, C., Vicca, S., Fisher, J. B., Reich, P. B., Stocker, B. D., Hungate, B. A., Peñuelas, J., McCallum, I., Soudzilovskaia, N. A., Cernusak, L. A., Talhelm, A. F., Van Sundert, K., Piao, S., Newton, P. C. D., Hovenden, M. J., ... Franklin, O. (2019). Nitrogen and phosphorus constrain the CO₂ fertilization of global plant biomass. *Nature Climate Change*, 9(9), 684–689. <https://doi.org/10.1038/s41558-019-0545-2>
- Tipping, R. (1995). Holocene evolution of a lowland Scottish landscape: Kirkpatrick Fleming. Part I, peat and pollen-stratigraphic evidence for raised moss development and climatic change. *The Holocene*, 5(1), 69–81. <https://doi.org/10.1177/095968369500500108>

- Valdes, P. J., Armstrong, E., Badger, M. P. S., Bradshaw, C. D., Bragg, F., Crucifix, M., Davies-Barnard, T., Day, J. J., Farnsworth, A., Gordon, C., Hopcroft, P. O., Kennedy, A. T., Lord, N. S., Lunt, D. J., Marzocchi, A., Parry, L. M., Pope, V., Roberts, W. H. G., Stone, E. J., ... Williams, J. H. T. (2017). The BRIDGE HadCM3 family of climate models: HadCM3@Bristol v1.0. *Geoscientific Model Development*, 10(10), 3715–3743. <https://doi.org/10.5194/gmd-10-3715-2017>
- Waddington, J. M., Morris, P. J., Kettridge, N., Granath, G., Thompson, D., & Moore, P. (2015). Hydrological feedbacks in northern peatlands. *Ecohydrology*, 8, 113–127.
- Wang, S., Zhang, Y., Ju, W., Chen, J. M., Ciais, P., Cescatti, A., Sardans, J., Janssens, I. A., Wu, M., Berry, J. A., Campbell, E., Fernández-Martínez, M., Alkama, R., Sitch, S., Friedlingstein, P., Smith, W. K., Yuan, W., He, W., Lombardozzi, D., ... Peñuelas, J. (2020). Recent global decline of CO₂ fertilization effects on vegetation photosynthesis. *Science*, 370(6522), 1295–1300. <https://doi.org/10.1126/science.abb7772>
- Wright, E. L., Black, C. R., Cheesman, A. W., Turner, B. L., & Sjögersten, S. (2013). Impact of simulated changes in water table depth on ex situ decomposition of leaf litter from a neotropical peatland. *Wetlands*, 33(2), 217–226. <https://doi.org/10.1007/s13157-012-0369-6>
- Wüst, R. A. J., Jacobsen, G. E., von der Gaast, H., & Smith, A. M. (2008). Comparison of radiocarbon ages from different organic fractions in tropical peat cores: Insights from Kalimantan, Indonesia. *Radiocarbon*, 50(3), 359–372. <https://doi.org/10.1017/S0033822200053492>
- Young, D. M., Baird, A. J., Gallego-Sala, A. V., & Loisel, J. (2021). A cautionary tale about using the apparent carbon accumulation rate

(aCAR) obtained from peat cores. *Scientific Reports*, 11(1), 9547. <https://doi.org/10.1038/s41598-021-88766-8>

Young, D. M., Baird, A. J., Morris, P. J., & Holden, J. (2017). Simulating the long-term impacts of drainage and restoration on the ecohydrology of peatlands. *Water Resources Research*, 53(8), 6510–6522. <https://doi.org/10.1002/2016WR019898>

SUPPORTING INFORMATION

Additional supporting information can be found online in the Supporting Information section at the end of this article.

How to cite this article: Young, D. M., Baird, A. J., Morris, P. J., Dargie, G. C., Mampouya Wenina, Y. E., Mbemba, M., Boom, A., Cook, P., Betts, R., Burke, E., Bocko, Y. E., Chadburn, S., Crabtree, D. E., Crezee, B., Ewango, C. E. N., Garcin, Y., Georgiou, S., Girkin, N. T., Gulliver, P. ... Lewis, S. L. (2023). Simulating carbon accumulation and loss in the central Congo peatlands. *Global Change Biology*, 00, 1–16. <https://doi.org/10.1111/gcb.16966>